Carbohydrate Polymers 363 (2025) 123738

Contents lists available at ScienceDirect

Carbohydrate Polymers

journal homepage: www.elsevier.com/locate/carbpol

Structural characterization and *in vitro* gut microbiota fermentation of a polysaccharide extracted from *Cenostigma nordestinum* gum

Francisca Crislândia Oliveira Silva [a], Maria Isabela Ferreira de Araújo [a], Soraia P. Silva [b], Elisabete Coelho [b], Aline Teixeira dos Santos [c], Abigail González [d], Andreia Filipa Ferreira Salvador [d,e], Thiago Barbosa Cahú [f], Angélica Thomaz Vieira [g], Marthyna Pessoa de Souza [h], Manuel A. Coimbra [b], José A. Teixeira [d,e], Clarisse Nobre [d,e,*], Paulo Antônio Galindo Soares [a,**], Maria Tereza dos Santos Correia [a,**]

[a] *Federal University of Pernambuco, Department of Biochemistry, Av. Prof. Moraes Rego s/n, CEP 50670-420 Recife, PE, Brazil*
[b] *LAQV-REQUIMTE, Department of Chemistry, University of Aveiro, 3810-193 Aveiro, Portugal*
[c] *Federal University of Ceara, Organic and Inorganic Chemistry Department, Av. Humberto Monte s/n, 60440-900, Fortaleza, CE, Brazil*
[d] *Centre of Biological Engineering (CEB), University of Minho, 4710-057 Braga, Campus de Gualtar, Portugal*
[e] *Associate Laboratory (LABBELS), University of Minho, Braga, Guimarães, Portugal*
[f] *Federal University of Rio de Janeiro, Institute of Biophysics Carlos Chagas Filho, Av. Carlos Chagas Filho, 21941-913, Rio de Janeiro, RJ, Brazil*
[g] *Federal University of Minas Gerais, Department of Biochemistry and Immunology, Av. Antônio Carlos, 31270-901, Belo Horizonte, MG, Brazil*
[h] *Federal University of Campina Grande, Academic Unit of Veterinary Medicine, Rural Health and Technology Center, R. João Salvino de Medeiros, 58708-110, Patos, PB, Brazil*

ARTICLE INFO

Keywords:
Arabinogalactan
Chemical structure
Microbiota
Prebiotic

ABSTRACT

This study aims to structurally characterize a polysaccharide extracted from *Cenostigma nordestinum* gum (AGCn) and evaluate its prebiotic potential in human gut microbiota. AGCn, obtained by dissolution in water and precipitation in 70 % ethanol, was primarily composed of carbohydrates (93.61 %), with a low protein content (1.70 %) and some phenolic compounds (9.16 % Gallic Acid Equivalents). Its molecular weight was 6.19×10^4 g/mol, with a dispersity of 1.33. The main monosaccharides identified were arabinose (38 mol%) and galactose (31 mol%). Methylation analysis and 2D NMR spectra showed that the gum exuded from *C. nordestinum* is a branched arabinogalactan composed of →6)-β-Gal*p*-(1→, →3,6)-β-Gal*p*-(1→, and →3,4,6)-β-Gal*p*-(1→ residues, containing chains of →3)-α-Ara*f*-(1→ and →5)-α-Ara*f*-(1→, with α-Ara*f*-(1→ and α-Rha*p*-(1→ as terminal residues. The identification of →4)-α-Gal*p*A-(1→ showed also the presence of a pectic polysaccharide. AGCn was metabolized by *Lactobacillus brevis*, *Lactobacillus plantarum*, and *Lactobacillus casei* probiotic bacteria. AGCn *in vitro* fermentation increased the ratio of *Bifidobacterium* and *Bacteroides* in the microbiota, decreased the abundance of bacteria associated with intestinal disease, and produced short-chain fatty acids. Thus, AGCn is an arabinogalactan with prebiotic potential as a gut microbiota modulator, offering significant value for future food and biotechnological applications.

1. Introduction

Gums exuded from plants are primarily composed of polysaccharides as their main structural component (Ahmadi et al., 2022; Zeng et al., 2022). Additionally, they contain, to a lesser extent, inorganic elements (Liu, Liu, et al., 2023), proteins (Chaudhari & Annapure, 2020, 2021; Liu, Zhao, et al., 2023), and phenolic compounds (Vasile et al., 2019). The degradation and complete absorption of polysaccharides in the human digestive system is a complex process influenced by their monosaccharides composition, type and stereospecificity of glycosidic bonds, degree of branching, and molecular weight (Wang et al., 2023). Undigested polysaccharides that escape digestion in the upper

* Correspondence to: C. Nobre, Centre of Biological Engineering (CEB), University of Minho, 4710-057, Braga, Campus de Gualtar, Portugal.
** Correspondence to: P.A.G. Soares and M.T.S. Correia, Federal University of Pernambuco, Department of Biochemistry, Av. Prof. Moraes Rego s/n, CEP 50670-420 Recife, PE, Brazil.
E-mail addresses: clarissenobre@ceb.uminho.pt (C. Nobre), paulo.gsoares@ufpe.br (P.A.G. Soares), maria.tscorreia@ufpe.br (M.T.S. Correia).

https://doi.org/10.1016/j.carbpol.2025.123738
Received 4 December 2024; Received in revised form 9 May 2025; Accepted 12 May 2025
Available online 14 May 2025
0144-8617/© 2025 Elsevier Ltd. All rights are reserved, including those for text and data mining, AI training, and similar technologies.

gastrointestinal tract reach the colon largely intact, where they are fermented by the gut microbiota (Bamigbade et al., 2022). Gut bacteria have a variety of carbohydrate-active enzymes (CAZymes) capable of degrading complex carbohydrates (Bamigbade et al., 2022; Elshahed et al., 2021). The metabolites produced during polysaccharide fermentation can modulate gut microbiota metabolism and influence species diversity (Liu et al., 2021). These effects may drive important strategies for developing new prebiotics aimed at modulating the gut microbiota (Mitra et al., 2023).

The gut microbiota is a large and diverse microbial community distributed in the colon, where it performs essential metabolic, structural, protective, and neurological functions that support host health (Adak & Khan, 2019; Portincasa et al., 2022; Sori et al., 2023). Changes in the composition of the gut microbiota, known as dysbiosis, are associated with genetic, physical, psychological, and environmental susceptibility factors, including diet, stress, frequent antibiotics use, and hormonal or immunological changes (Hooks & O'Malley, 2017; Talapko et al., 2022). This process is characterized by an imbalance and instability in bacterial colonization, which can triggers harmful effects on an individual's health (Mutuyemungu et al., 2023; NeuHannig et al., 2019). In this context, prebiotics have been explored as potential candidates for regulating gut microbiota composition.

Defined as non-digestible substrates that confer health benefits to the host, prebiotics can selectively stimulate the growth and/or metabolic activity of gut microbiota-associated bacteria (Gibson et al., 2017). The functional characteristics of prebiotics are associated with their ability to selectively promote the growth of probiotic bacteria, such as *Lactobacillus* and *Bifidobacterium*, while inhibiting the colonization of pathogenic bacteria. They also support anaerobic intestinal conditions that foster bacterial growth, lower pH levels, maintain intestinal barrier integrity, and enhance the production of short-chain fatty acids (SCFAs) (Munteanu & Schwartz, 2024). These combined functions contribute to the regulation of metabolism (Enam & Mansell, 2019; Portincasa et al., 2022). Carbohydrates such as fructo-oligosaccharides (FOS), galacto-oligosaccharides (GOS), and xylo-oligosaccharides (XOS) are among the most extensively investigated substrates with prebiotic action (Nobre et al., 2022). In addition, *in vitro* and *in vivo* experimental analyses have shown the potential prebiotic effect of plant gum polysaccharides (K-da et al., 2020; Silva et al., 2023).

Cenostigma nordestinum is an endemic plant native to the Caatinga phytogeographic domain, widely distributed in the Brazilian semi-arid region and popularly known as "catingueira," "catinga-de-porco," and "pau-de-rato" (Soares et al., 2022). *C. nordestinum* is often confused with *Cenostigma pyramidale*, previously described as *Caesalpinia pyramidalis* or *Poincianella pyramidalis*, due to the shared popular name, "catingueira." This confusion arises from the similar characteristic unpleasant odor present in both species, which belong to the same Fabaceae family (Rodrigues et al., 2020; Soares et al., 2022). In addition, the plant parts of *C. nordestinum*, such as bark, flowers, and leaves, treat pyelonephritis, hepatitis, hypertension, and gastrointestinal disorders (de Sousa et al., 2021). Studies on its chemical constituents have identified a range of metabolite compounds in its leaves, bark, and bark exudate, including polysaccharides, phenolics, alkaloids, flavonoids, flavanones, tannins, and xanthones (Soares et al., 2022).

Despite the wide range of bioactive compounds identified and characterized in the plant parts of *C. nordestinum*, the structural composition and the biological potential of the polysaccharide obtained from its gum have not yet been explored in scientific studies. Considering the plant association with gastrointestinal disorders treatment, this study hypothesizes that the polysaccharide from the *C. nordestinum* gum presents prebiotic potential. Therefore, the objective of this work was the structural characterization of the polysaccharide obtained from *C. nordestinum* gum and the evaluation of its prebiotic potential in modulating the intestinal microbiota through *in vitro* faecal fermentation.

2. Materials and methods

2.1. Chemicals and reagents

Bovine serum albumin (BSA), δ-glucuronolactone, gallic acid, L-rhamnose (Rha), L-arabinose (Ara), D-mannose (Man), D-galactose (Gal), D-glucose (Glc), D-xylose (Xyl), D-galacturonic acid (GalA), Porcine pepsin, pancreatin, bile extract, pefabloc SC, $(NH_4)_2CO_3$, $NaHCO_3$ and HCl (37 %, *w/v*) were purchased from Sigma-Aldrich Chemical Co. (St. Louis, MO, USA). $MgCl_2{\cdot}(H_2O)_6$ was pure pursued from Merck (Germany). NaCl, KCl, NaOH, KH_2PO_4, and $CaCl_2{\cdot}(H_2O)_2$ were obtained from Panreac (Spain). P-82 pullulan standards were obtained from Shodex Denko® (Tokyo, Japan). The lactate standards and Short Chain Fatty Acids (SCFAs) (Acetic, Propionic, Iso-Butyric, and Formic) were purchased from Aladdin Industrial Inc. (Shanghai, China). All other reagents were of analytical grade.

2.2. Plant material

The gum exuded from *C. nordestinum* was collected in the municipality of Patos, Paraíba, Brazil (7° 03′33.3″S37°16′30 0″ W). Botanical identification was then performed and the exsiccates were deposited in the Rita Baltazar de Lima Herbarium of the Federal University of Campina Grande (UFCG) under registration number 7458. The plant species was registered under the access number ABF5334 in the National System for the Management of Genetic Heritage and Associated Traditional Knowledge (SisGen) of the Ministry of the Environment (Brazil).

2.3. Extraction and purification of gum polysaccharide

The polysaccharide from *C. nordestinum* gum was extracted according to the methodology of Souza et al. (2010), with minor modifications. Briefly, the gum was grounded and dissolved in distilled water (20 % *w/v*) under magnetic stirring (200 rpm/min) during 2 h at room temperature (25 °C). The solution was filtered using cheesecloth, followed by further filtration on a silk tissue (90 threads). The filtrate was precipitated for 18 h with absolute ethanol to a final concentration of 70 % (*v/v*), centrifuged (2.800 ×*g*; 15 min), freeze-dried, and finally pulverized with the aid of a knife mill to obtain the powdered polysaccharide extracted from the gum of *C. nordestinum* (AGCn). This procedure was performed in triplicate to estimate the yield of the extraction as the ratio of the final mass of the precipitate powder (m_f) to the initial mass of the gum (m_i), which was expressed as % (*w*/w).

2.4. Chemical and structural characterization of AGCn

2.4.1. Colorimetric chemical analyses

The total sugar content was determined according to modifications of the phenol-sulfuric acid methodology by adding 2–40 μL of sample dissolved in distilled water (0.005–0.1 mg/mL), followed by 20 μL of 80 % (*w/v*) phenol and 1 mL of 97 % sulfuric acid. After 30 min, the absorbance of the samples was measured at λ = 490 nm using a UV/Visible spectrophotometer (Amersham Biosciences Ultrospec 3100 pro). A galactose standard curve (0.005–0.1 mg/mL) was prepared and subjected to the same procedure (Coelho et al., 2020).

Spectrophotometric analysis was applied to determine the total protein (Bradford, 1976) and phenolic contents (Singleton & Rossi Jr., 1965) using bovine serum albumin (A_{595} nm) and gallic acid (A_{765} nm) as standards, respectively. The uronic acid content was measured according to modifications in 3-phenylphenol colorimetric method. The polysaccharide was hydrolysed with 1 mol/L of H_2SO_4, for 1 h at 100 °C and the uronic acids quantified as galacturonic acid equivalents. A calibration curve was prepared using D-galacturonic acid as standard and then measured at 520 nm. All samples were analyzed in triplicate (Gudiña et al., 2023).

2.4.2. Gel permeation chromatography (GPC)

The peak molecular weight (Mp), average molecular weight (Mw), number average molecular weight (Mn) and dispersity (D) distribution of AGCn was determined by Gel Permeation Chromatography (GPC) using a Shimadzu LC-20AD chromatograph coupled to a refractive index detector (RID-10A) (Lima et al., 2021; Pereira et al., 2021). AGCn was dissolved in deionized water (1 mg/mL; 0.1 % *w/v*), and 50 μL of this solution was applied to a linear PolySep column (7.8 × 300 mm) working with a mobile phase of 0.1 mol/L $NaNO_3$, at room temperature (25 °C), and a flow rate of 1 mL/min. To determine the Mp, Mw, Mn, and D of AGCn, a calibration curve was established using pullulan standards (Shodex Denko®) with a molecular weight ranging from 5.9×10^3 to 7.88×10^5 g/mol.

2.4.3. UV–visible and Fourier transform infrared (FTIR) spectroscopy analysis

The ultraviolet spectrum of AGCn (2 mg/mL mg) was performed using a UV–Vis spectrophotometer (Ultrospec 2100 pro, Amersham Biosciences) in the wavelength range of 200–700 nm. The FT-IR spectrum of AGCn (5 mg) was taken in an ATR (Attenuated Total Reflection) window and analyzed in the wavelength range from 500 to 4000 cm^{-1} with a resolution of 4 cm^{-1} and the average measurement of 120 scans (Perkin Spectrophotometer Elmer) (de Araujo et al., 2021).

2.4.4. Monosaccharide composition

The monosaccharide composition of AGCn was obtained by treatment with 72 % (*w/w*) H_2SO_4 for 3 h at room temperature with occasional stirring followed by hydrolysis with 1 mol/L H_2SO_4 for 2.5 h at 100 °C. Monosaccharides were reduced with $NaBH_4$ (15 % in 3 M NH_3) for 1 h at 30 °C and subsequently acetylated with acetic anhydride (3 mL) in the presence of 1-methylimidazole (450 μL) for 30 min at 30 °C. The alditol acetate derivatives were separated with dichloromethane and analyzed by Gas chromatography with a flame ionization detector (GC-FID) (Perkin Elmer-Clarus 400) and equipped with a 30 m DB-225 column (J&W Scientific, Folsom, CA, USA) with *i.d.* and film thickness of 0.25 mm and 0.15 μm, respectively (Hamed et al., 2022). The results were compared with analytical standards for arabinose, galactose, glucose, mannose, rhamnose, and xylose, submitted to the same procedures.

2.4.4.1. Glycosidic linkage analysis. The glycosidic linkage composition of AGCn was determined by methylation analysis. The AGCn (1–2 mg) was dissolved in 1 mL of dimethyl sulfoxide, and then NaOH powder (40 mg) was added under argon atmosphere. The samples were methylated with CH_3I (80 μL) for 20 min with stirring, followed by a second addition of 80 μL of CH_3I and stirring for another 20 min. $CHCl_3$/MeOH (1:1 *v/v*; 3 mL) was added, and the solution was dialyzed (12 kDa) against 50 % EtOH. The remethylated material was hydrolyzed with 2 M trifluoroacetic acid (1 mL) at 120 °C for 1 h and then reduced and acetylated with $NaBD_4$. The partially methylated alditol acetates (PMAA) were separated and analyzed by Gas Chromatography Coupled to Mass Spectrometry (GC–MS QP2010 Ultra, coupled to a QP2010 Ultra) (Shimadzu). The mass profile of the PMAA fragments was compared with the same monosaccharide standards with different methylation profiles (Bastos et al., 2015).

2.4.5. Nuclear magnetic resonance spectroscopic analysis

The ^1H and ^{13}C NMR spectra of the AGCn were recorded using a Varian VNMRS-500 MHz spectrometer with a triple resonance probe, as described by de Araujo et al. (2021). Approximately 10 mg of the sample was dissolved in 0.6 mL of 99.6 % deuterium oxide (D_2O) as an external reference at 40 °C with D_2O suppression by pre-saturation. The 1D ^1H NMR spectrum was recorded with 16 scans. The 2D (^1H—^1H) TOCSY (Total Correlation Spectroscopy) spectrum was acquired with a spin-lock field of 10 kHz and a mixing time of 80 ms. ^1H—^{13}C multiplicity-edited HSQC (Edited Heteronuclear Single Quantum Correlation Spectroscopy) spectrum (1024 × 256 points) was acquired with globally optimized alternating rectangular phase pulses for decoupling. ^1H and ^{13}C chemical shifts were calibrated with the basis of signals from trimethylsilyl propionic acid as standard at 0 ppm. Spectra were processed using the software Top-Spin 3.6.5 (Bruker).

2.5. In vitro utilization of carbon sources by probiotic bacteria

Lactobacillus rhamnosus (CECT 278), *Lactobacillus brevis* (CECT 216), *Lactobacillus plantarum* (CECT 748), and *Lactobacillus casei* (ATCC 334) were gently provided by the Laboratory of Microorganism Genetics (LGMi) at the Federal University of Pernambuco. Lactobacilli cultures were kept at −80 °C in glycerol at 25 % (*v/v*). For prebiotic activity assays, the frozen cultures were cultured in Man-Rogosa-Sharpe (MRS) broth and incubated at 37 °C for 48 h.

The assays were performed according to a previous study (Nobre et al., 2018). MRS broth with a substituted carbon source was used to evaluate the prebiotic potential of AGCn. MRS broth without carbon source was autoclaved at 121 °C for 15 min and prepared according to the following formulation: 10 mg/mL peptone, 10 mg/mL meat extract, 5 mg/mL yeast extract, 2 mg/mL K_2HPO_4, 1.08 mg/mL Tween 80, 5 mg/mL $C_2H_3NaO_2$, 2 mg/mL tribasic ammonium citrate, 0.2 mg/mL $MgSO_4$, and 0.05 mg/mL $MnSO_4$. Solutions of inulin (INU), glucose (GLC), and AGCn were prepared and sterilized by filtration through 0.22 μm filters and used as a carbon source. Each solution was added separately to the MRS broth to reach a final concentration of 2 % (*w/v*) in the culture medium. Filter-sterilized distilled water was used as a negative control (NC).

The assays were performed by adding 2 % (v/v) of each probiotic strain to the MRS broth containing the different carbon sources. The inoculated media were transferred (300 μL) to a 96-well microplate. The microplate was incubated at 37 °C for 48 h. The optical density at 600 nm was recorded at a 12-h interval (1, 12, 24, 36, and 48 h) using a microplate reader. All assays were performed in triplicate.

2.6. In vitro faecal fermentation

Three healthy donors, aged between 25 and 35, provided fresh faecal samples. Participants received no antibiotic, probiotic, or prebiotic treatment for at least three months before the study. Each participant signed an informed consent form providing information about the study.

Faecal samples were collected in sterile plastic containers and stored in anaerobic conditions at 4 °C until delivery and processing (maximum 2 h after collection). Each sample was individually weighted in a sterile Stomacher® bag and diluted at 10 % (*w/v*) in Reduced Physiological Salt solution (RPS), which consisted of 0.5 mg/mL L-cysteine to act as a reducing agent and 0.5 mg/mL NaCl to maintain the osmotic balance of the medium (Rymovicz et al., 2011; Wang et al., 2024). A Nutrient Base Medium (NBM) was prepared according to Roupar et al. (2022). NBM with the addition of AGCn (previously filter-sterilized at 0.22 μm) at a final concentration of 2 % w/v was used as a sample test. A negative control (NBM without additional carbon source) was also prepared.

In vitro fermentations were conducted in a static batch model under anaerobic conditions (85 % N_2, 10 % CO_2, and 5 % H_2). Fermentation experiments were initiated by adding the prepared faecal inoculum at 2 % (*v/v*) to the anaerobic medium, followed by incubation at 37 °C. Samples were collected at 0, 12, 24, and 48 h fermentation. The pH value of the collected samples was measured using a pH meter (Orion Star A211, Thermo Fisher Scientific) to track bacterial growth and activity.

2.6.1. Carbohydrate and fermentation product analysis

During fermentation, the sugar concentration was analyzed by gas chromatography with flame ionization detection (GC-FID) and levels of organic acids (lactate and SCFAs) were calculated by high-performance

liquid chromatography (HPLC). Aliquots collected during fermentation (0, 12, 24, and 48 h) were centrifuged (11.200 ×*g*; 6 min). The supernatant was used to determine the total of carbohydrates and organic acids. The resulting pellet was used for genomic DNA extraction for subsequent gut microbiota analysis.

Neutral sugars were released from the AGCn sample by chemical treatment with 200 μL of 72 % (*w*/w) H_2SO_4 for 3 h at room temperature, with occasional stirring, followed by hydrolysis with 1.0 mol/L H_2SO_4 for 2.5 h at 100 °C using heating block. Samples were neutralized with 25 % NH_3 and then reduced with acetic anhydride (3 mL) in the presence of 1-methylimidazole (450 μL) for 30 min at 30 °C. Alditol acetate derivatives were separated using dichloromethane and analyzed by Gas Chromatography with Flame Ionization Detection (GC-FID) (Perkin Elmer–Clarus 400) equipped with a 30 m DB-225 (J&W Scientific, Folsom, CA, EUA) with i.d. and film thickness of 0.25 mm and 0.15 μm, respectively. Samples were analyzed in triplicate (Bastos et al., 2015).

For the quantification of lactic acid and SCFAs, an HPLC system equipped with an Aminex HPX-87H chromatographic column (8 μm, 30 cm × 0.46 cm length × diameter) coupled with a UV detector (wavelength: 210 nm) was used. Samples were eluted in a sulfuric acid (5 mM) solution at a 0.6 mL/min flow rate and 60 °C (Roupar et al., 2023). The chromatographic signal was recorded and further integrated using the Star Chromatography Workstation 6.3 software (Varian, CA, USA). SCFA and lactic acid standards were obtained from Merck.

2.6.2. Analysis of gut microbiota

The gut microbiota composition was analyzed at 0 h for the basal (initial composition of the gut microbiota) and after 24 h of fermentation for the INU and AGCn groups. The total bacterial DNA was extracted using a NZY Tissue gDNA Isolation Kit (Nzytech, Portugal) according to the manufacturer's instructions. Briefly, faecal samples were centrifuged at 10,000 ×*g* for 10 min to separate the supernatant from the pellet. Then, the pellets were homogenized in 1 mL of Tromethamine-Ethylenediamine Tetraacetic Acid (Tris-EDTA) buffer (10 mM Tris/HCl; 1 mM EDTA, pH 8.0) and centrifuged (4000 ×*g*, 15 min, 4 °C). The supernatant was discarded, and the pellet was resuspended in 500 μL of Tris-EDTA buffer, with subsequent centrifugation (4000 ×*g*, 15 min, 4 °C). This process was repeated twice. The supernatant was discarded, and the pellet was resuspended in 180 μL of lysozyme (10 mg/mL dissolved in NaCl (30 mM) and EDTA (10 mM)) and incubated for 1 h at 37 °C (Roupar et al., 2022).

After extraction, the bacterial DNA concentration and purity were assessed through a NanoDrop spectrophotometer (Thermo Scientific, Wilmington, DE, USA). Sequencing of the prokaryotic 16S rRNA gene, V4 region, was performed by RTL Genomics (Lubbock, TX, USA) on the Illumina MiSeq platform (Illumina Inc., San Diego, CA, USA) by using the primer pair 515F/806R (515F: GTGCCAGCMGCCGCGGTAA; 806R: GGACTACHVGGGTWTCTAAT). The sequencing data were further analyzed using the Quantitative Insights into Microbial Ecology (QIIME) pipeline (Boulder, CO, USA) and the Ribosomal Database Project (East Lansing, MI, USA). All results were based on the sequenced reads and operational taxonomic units (OTUs) at 97 % sequence similarity. Taxonomy assignment of OTUs was performed by comparing sequences to the Greengenes database (Berkeley, CA, USA).

2.7. Statistical analysis

All experimental procedures were performed in triplicate, and results were expressed as mean ± standard deviation. Means were compared using Analysis of Variance (ANOVA) followed by a one-way test using GraphPad Prism software version 8.0 (Inc., California, USA). Statistical data was considered significant at $p < 0.05$, where capital letters indicate differences between experimental groups between fermentation times, and lowercase letters indicate differences between experimental groups.

3. Results and discussion

3.1. Purification and characterization of AGCn

The methods commonly described in the literature for extracting plant gum polysaccharides mainly involve aqueous extraction, followed by purification through ethanol precipitation (De et al., 2020; Sharma et al., 2021). The addition of ethanol reduces the polarity of the aqueous medium. Polysaccharides, generally polar due to the hydroxyl groups (OH) in their structures, become less soluble in a medium with lower polarity. Consequently, the polysaccharides clump together, forming a polysaccharide precipitate (Tai et al., 2020). Based on the described methodology, the ethanol extract obtained from AGCn provided a yield of 38.40 ± 4.67 % relative to the initial dry mass of the gum (Table 1). Regarding the chemical composition, AGCn exhibited a concentration of 93.61 ± 0.63 % total carbohydrates, including 11.50 ± 0.37 % uronic acid, a low content of proteins (1.70 ± 0.28 %) and phenolic compounds (9.16 ± 0.02 %/EGA) (Table 1).

The purification methodology used to obtain AGCn resulted in an intermediate yield compared to data found in the literature, where variations in yield range from 16.50 % to 77.44 % among polysaccharides extracted from *Piptadeniastrum africana*, *Acacia tortilis*, *Soymida febrifuga*, *Khaya senegalensis* and *Grewia mollis* gums (Bhushette & Annapure, 2018; Chaudhari & Annapure, 2021; Eshun Oppong et al., 2021; Lakhera & Kumar, 2017). Furthermore, the chemical composition of AGCn revealed a high degree of gum purity, proving the efficiency of the purification method (Chaudhari & Annapure, 2021), with similar results found for the polysaccharides extracted from *Prunus domestica* (Sharma et al., 2020), *Prangos ferulacea* (Kheradkhord & Shekarchizadeh, 2022), and *Prosopis alba* (Vasile et al., 2019) gums.

Table 1
Yield, chemical characterization, and gel permeation chromatographic analysis (GPC) of arabinogalactan extracted from *Cenostigma nordestinum* gum (AGCn).

Concentration (%)[a]	
Yield	38.40 ± 4.67
Chemical characterization (*w*/w%)[b]	
Total sugars	93.61 ± 0.63
Protein	1.70 ± 0.28
Phenolic compounds[c]	9.16 ± 0.02
Monosaccharide residues composition (mol %)[d]	
Rhamnose	7
Arabinose	38
Xylose	2
Mannose	1
Galactose	31
Glucose	2
Uronic acids	19
Gel Permeation Chromatography (g/mol)[e]	
Mp	6.19×10^4
Mw	8.35×10^4
Mn	6.29×10^4
D (Mw/Mn)	1.33

[a] % relative to dry sample weight.
[b] w % total weight of the compounds/w % relative to dry weight.
[c] %/GAE-gallic acid equivalent %.
[d] Based on GC-FID analysis of alditol acetates (Mol % relative to the total amount of neutral monosaccharide residues of AGCn).
[e] Molecular weights: Peak (Mp), Average (Mw), Numerical (Mn), and Dispersity (D) of AGCn by Gel Permeation Chromatography.

Polysaccharides are naturally polydisperse polymers, as they exhibit an average molecular weight representing a distribution of molecular species nearly identical in structure but vary in chain length (Pereira et al., 2021). A characteristic polydispersity of the molecular weight profile of AGCn by GPC showed a single and partially sharp peak (Supplementary material; Fig. S1A), indicating that AGCn is a homogeneous polysaccharide. According to the calibration curve using pullulan standards (Supplementary material; Fig. S1B), the peak molecular weight (Mp), average (Mw), and numerical (Mn) of AGCn were approximately 6.19×10^4, 8.35×10^4, and 6.29×10^3 g/mol, respectively. In addition, the dispersity value (D) of AGCn, calculated by the Mw/Mn ratio, was 1.33×10^1 g/mol (Table 1). This set of analytical data clearly demonstrates the purity and homogeneity of AGCn (Soares et al., 2018), and the molecular weight values are considered comparable to those obtained for the polysaccharide extracted from *Anacardium occidentale* gum (Melo et al., 2020).

UV–visible spectroscopy is widely used to analyse chromophoric groups characterized by strong absorption of electronic transitions (Zhou et al., 2022). In the UV–visible spectrum of AGCn (Supplementary material; Fig. S2A), the maximum absorption was observed at 220 nm, corresponding to transitions related to functional groups such as carboxyl, carbonyl, and ester groups (Trabelsi et al., 2009). Furthermore, no absorbance peak was detected at 260 and 280 nm, indicating the low presence of proteins and nucleic acid (de Araujo et al., 2021), which is also consistent with the chemical analysis of AGCn. The absorption infrared spectra of AGCn (Supplementary material; Fig. S2B) exhibited characteristic spectra of polysaccharides extracted from plant gums (Bhushette & Annapure, 2018; Chaudhari & Annapure, 2021; Eshun Oppong et al., 2021; Sharma et al., 2021).

The monosaccharide composition data of AGCn was determined based on the analysis of alditol acetates formed after acid hydrolysis (Hamed et al., 2022). The analysis revealed the presence of arabinose (38 %) and galactose (31 %) as the main constituent sugars, followed by a concentration of 19 % uronic acid. In smaller proportions, rhamnose (7 %), xylose (2 %), glucose (2 %), and mannose (1 %) were also detected (Table 1). This is in accordance with the fact that the polysaccharides of exudate gums from plants have been identified as arabinogalactans, primarily composed of arabinose and galactose as the main sugars (Sharma et al., 2020).

The glycosidic linkage analysis performed by methylation of AGCn (Table 2) showed that the Ara residues were Ara*f*-(1→ (28.8 %), →3)-Ara*f*-(1→ (14.1 %), and →5)-Ara*f*-(1→ (4.7 %)), and the Gal residues were mainly →3,6)-Gal*p*-(1→ (17.3 %), →6)-Gal*p*-(1→ (12.0 %), and →3,4,6)-Gal*p*-(1→ (8.3 %). To a lesser extent, Rha*p*-(1→ terminal bonds were present (1.4 %).

The glycosidic bonds of AGCn show characteristics of an arabinogalactan, which is also supported by the literature on arabinogalactans from plant gums (Ahmadi et al., 2022), such as those from *Prunus persica* (Wei et al., 2023), *Dorema ammoniacum* (Ahmadi et al., 2022), *Odina wodier* (De et al., 2020), and *Albizia stipulata* (Thanzami et al., 2015). The predominant presence of arabinose and galactose residues and respective glycosidic linkages reinforce the classification of AGCn as an arabinogalactan, a polysaccharide widely found in plant exudates, as also found in species of *Prunus persica* and *Lycium barbarum* (Wei et al., 2023). Furthermore, the presence of branched galactose residues such as →3,6)-Gal*p*-(1→ and →3,4,6)-Gal*p*-(1→ suggests a branched structure.

The ^{1}H and ^{13}C NMR assignments obtained from the combination of TOCSY (^{1}H/^{1}H) and HSQC (^{1}H/^{13}C) spectra of AGCn are shown in Table 3 and in Supplementary material; Fig. S3. The signals in the anomeric region between δ 5.1 to δ 5.8 in ^{1}H NMR for Ara and GalA, and between δ 4.79 for terminal Rha strongly indicate the presence of sugar residues with α configuration, while those characteristic of β configuration, namely Gal, generally appear in δ 4.4 to 4.6 ^{1}H NMR (Tan et al., 2004; Yao et al., 2021). In addition, H6/C6 peaks observed in the δ 1.1 to 1.33 region in ^{1}H NMR and δ 16 to 22 in ^{13}C NMR suggest the presence of the methyl group of rhamnose (Nunes et al., 2008).

The TOCSY spectrum (Fig. 1A) shows the correlations between protons that are in a chain of coupled protons and that interrelate through the propagation of magnetization (spin-lock sequence) (Speciale et al., 2022), while the HSQC spectrum (Fig. 1B) establishes the heteronuclear correlation of the frequency of proton and carbon signals in the molecule (Mauri et al., 2017).

The 1D and 2D NMR spectra analysis showed the chemical shift signals attributed to the AGCn residues. The signals of the main chain of AGCn were obtained at $\delta H/\delta_C$ 4.52/104.23, 3.67/73.10, 3.81/71.10, 3.73/70.70, 3.91/74.54, 3.68/70.90 ppm, respectively, in H-1/C-1 to H-6/C-6 of residue E. These values correspond to the characteristic proton and carbon pattern of the →6)-β-Gal*p*-(1→ residue attributed to the main chain in the structural composition of arabinogalactans (Wei et al., 2023). The downward shift of the C-3 (80.05 ppm) and C-6 (70.76 ppm) signals refers to the residues of the β-Gal*p* AGCn side chain linked at C-3 and C-6 of the D main chain (Fig. 1A and B) (Ahmadi et al., 2022).

The chemical shift values of the C residue correspond to the signals at

Table 2
Glycosidic linkage composition determined for the arabinogalactan extracted from *Cenostigma nordestinum* gum (AGCn).

Residue identified by NMR	Glycosidic linkage	mol (%)[a]
G	α-Rha*p*-(1→	1.4
A	α-Ara*f*-(1→	28.8
–	→2)-Ara*f*-(1→	0.3
B	→3)-Ara*f*-(1→	14.1
C	→5)-Ara*f*-(1→	4.7
–	→2,5)-Ara*f*-(1→	1.2
–	→3,5)-Ara*f*-(1→	0.5
–	Xyl*p*-(1→	2.7
–	→4)-Xyl*p*-(1→	1.0
–	Gal*p*-(1→	1.0
–	→3)-Gal*p*-(1→	3.9
–	→4)-Gal*p*-(1→	1.1
E	→6)-β-Gal*p*-(1→	12.0
D	→3,6)-β-Gal*p*-(1→	17.3
–	→4,6)-Gal*p*-(1→	0.2
F	→3,4,6)-β-Gal*p*-(1→	8.3
–	→2,3)-Glc*p*-(1→	0.9
–	→3,4)-Glc*p*-(1→	0.6

[a] % mol in relation to the amount of glycosidic linkage residues of AGCn based on GC–MS analysis of partially methylated alditol acetates. Capital letters identify the residues assessed by NMR, allowing to assign their anomeric configuration.

Table 3
^{13}C and ^{1}H NMR data of arabinogalactan extracted from *Cenostigma nordestinum* (AGCn) gum.

Residue	Sugar linkage	Chemical shifts (ppm)[a]					
		H-1 C-1	H-2 C-2	H-3 C-3	H-4 C-4	H-5 C-5	H-6 C-6
A	α-Ara*f*-(1→	5.10 108.05	4.12 82.30	3.81 79.46	4.04 83.84	3.67 61.53	–
B	→3)-Ara*f*-(1→	5.10 107.80	4.11 83.21	3.91 83.94	3.81 83.00	3.67 63.41	–
C	→5)-Ara*f*-(1→	5.25 109.43	4.23 83.24	3.91 76.53	3.68 83.84	3.82 70.71	–
D	→3,6)-β-Gal*p*-(1→	4.42 103.50	3.55 74.50	3.73 80.05	4.13 69.00	3.91 74.61	3.81 70.76
E	→6)-β-Gal*p*-(1→	4.52 104.23	3.67 73.10	3.81 71.10	3.73 70.70	3.91 74.54	3.68 70.90
F	→3,4,6)-β-Gal*p*-(1→	4.46 105.01	3.73 73.40	3.90 85.00	3.99 86.70	3.65 75.7	4.06 72.4
G	α-Rha*p*-(1→	4.77 101.64	3.92 70.92	3.75 71.18	3.43 73.51	4.04 69.34	1.26 16.70
H	→4)-α-Gal*p*A-(1→	5.44 101.90	4.10 70.67	4.00 70.20	Nd	nd	nd

[a] The data were obtained from 1D ^{1}H NMR spectra and the combination of TOCSY (^{1}H/^{1}H) and HSQC (^{1}H/^{13}C) spectra at 500 MHz. The chemical shifts are based on Tetramethylsilane - TMS. nd – not detected.

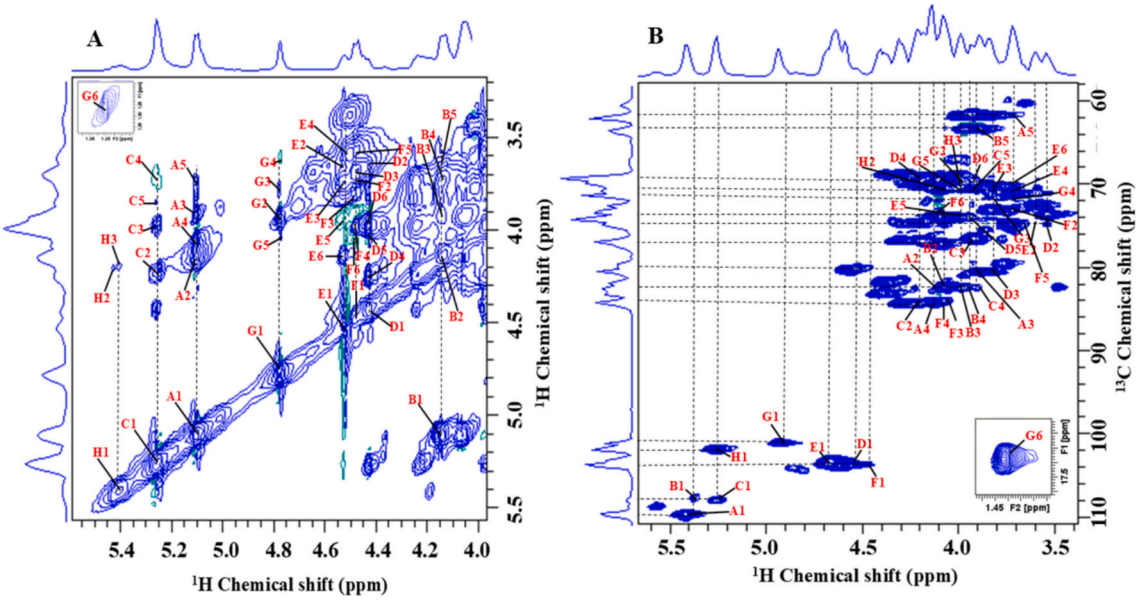


Fig. 1. NMR spectra of the arabinogalactan extracted from *Cenostigma nordestinum* gum (AGCn) recorded at 25 °C on a Varian VNMRS-500 spectrometer at 500 MHz. (A) Strip from the ^{1}H—^{1}H TOCSY spectra of AGCn. (B) ^{1}H—^{13}C HSQC spectra of AGCn.

5.25/109.43, 4.23/83.24, 3.91/76.53, 3.68/83.84, and 3.82/70.71 ppm, assigned respectively to H-1/C-1 to H-5/C-5 (Table 3). The C-5 signals at 70.71 ppm indicated that the C residue was α-Ara*f* (1 → 5)-linked (Fig. 1A and B) (Hamed et al., 2022; Li et al., 2020). The δ_C signals at 101.90/70.67/70.20 ppm refer to the galacturonic acid residue bound to carbon 4 (G) (Fig. 1B), while the δ_H signals of these residues are obtained at 5.26/4.10/4.00 ppm (Fig. 1A) (Coelho et al., 2020; Hamed et al., 2022). This is in accordance with the reported structures for the polysaccharides of gums from the *Astragalus* genus, which have a high proportion of C-4-linked galacturonic acid (Gavlighi et al., 2013).

Branched arabinogalactans were confirmed by the residues →3,6)-β-Gal*p*-(1 → (D) and →3,4,6)-β-Gal*p*-(1 → (F), according to the intense and high H/C correlations of typical β-pyranose at δ 4.42/103.50 (D), δ 4.52/104.23 (E) and a weak one at δ 4.46/105.01 (F) in the TOCSY (Fig. 1A) and HSQC (Fig. 1B) (Fu et al., 2022).

The terminal residues such as α-Ara*f*-(1→ showed strong signals at 5.10/108.05 ppm attributed to protons and anomeric carbons (H-1 and C-1), while the signals at 3.67/61.53 related to H-5 and C-5 are strongly attributed to the terminal α-Ara*f*-(1→ (Li et al., 2022). The other terminal residue α-Rha*p*-(1→ obtained characteristic δH/δ_C signals at 4.77/101.64, 3.92/70.92, 3.75/71.18, 3.43/73.51 and 4.04/69.34 ppm assigned to H-1/C-1 to H-5/C-5 of the residue. The signals detected at 1.26 ppm and 16.70 ppm are assigned to the H-6/C-6 methyl group of α-Rha*p*-(1→ (Table 3; Fig. 1B) (Ahmadi et al., 2022; Wu et al., 2020). In addition, the terminally linked α-Rha*p*-(1→ residues may represent the non-reducing ends of the side chains and may be linked to arabinose residues, as reported by Hamed et al. (2022). Therefore, according to the structural characteristics, signals of the glycosidic residues obtained by methylation and NMR analysis, and a comprehensive literature review, it was possible to establish that AGCn is a polysaccharide of the acid arabinogalactan type with a main chain →6)-β-Gal*p*-(1→ branched at →3,6)-β-Gal*p*-(1→ and →3,4,6)-β-Gal*p*-(1→ with branches of terminally-linked α-Ara*f*, and side chains of residues of 3-α-Ara*f* and 5-α-Ara*f*. Also, →4)-α-Gal*p*A-(1→ was assigned, probably linked to the arabinogalactan in a rhamnogalacturonan type I region *via* a rhamnose residue. A terminally-linked residue of α-Rha*p* was assigned.

Taking into account that based on the TOCSY and HSQC spectra and supported by methylation analysis, the glycosidic residues assigned for α-Ara*f*-(1→ (A), →3)-α-Ara*f*-(1→ (B), →5)-α-Ara*f*-(1→ (C), →3,6)-β-Gal*p*-(1→ (D), →6)-β-Gal*p*-(1→ (E), →3,4,6)-β-Gal*p*-(1→ (F), α-Rha*p*-(1→ (G), and →4)-α-Gal*p*A-(1→ (H), the AGCn gum analyzed seem to be an arabinogalactan together with a small portion of a pectic polysaccharide. Based on the results presented, the proposed structure of AGCn is shown in Fig. 2, comprising a main chain of →6)-β-Gal*p*-(1→ (Zhang et al., 2020).

3.2. Grow of probiotic bacteria in AGCn

The results of the growth of *Lactobacillus* strains (*L. rhamnosus*, *L. brevis*, *L. plantarum* and *L. casei*) in medium containing no carbon source (NC), glucose, inulin or AGCn are shown in Fig. 3. As expected, all microorganisms grew in the medium containing glucose and inulin as carbon sources (positive controls), showing increased cell density from 12 to 48 h. Furthermore, none of the *Lactobacillus* strains was able to grow without carbohydrate supplementation, as observed in the negative control (Fig. 3). In the studies by Nobre et al. (2018) and Wang, Pan, et al. (2020), the controls groups (negative and positive) also exerted the same effects on the growth of *Lactobacillus* strains. Nobre et al. (2019) also demonstrated that the strains of *Lactobacillus* tested in this study could grow using glucose as the preferred carbon source without

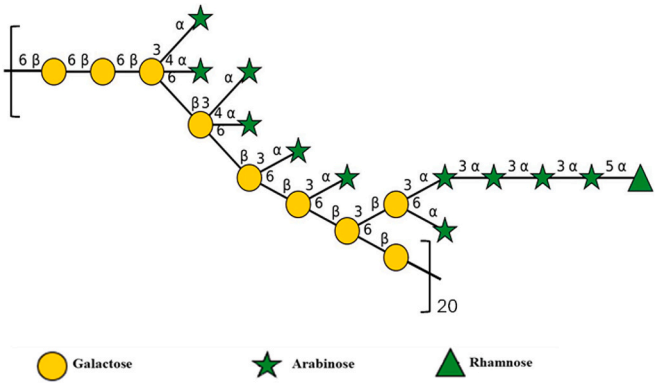


Fig. 2. Schematic tentative structure of the arabinogalactan extracted from *Cenostigma nordestinum* gum based on glycosidic linkage analysis and the estimated molecular weight, obtained from the structure editor of the Carbohydrate Structure Database using the Symbol Nomenclature for Glycans - CSDB/SNFG (Cheng et al., 2017).

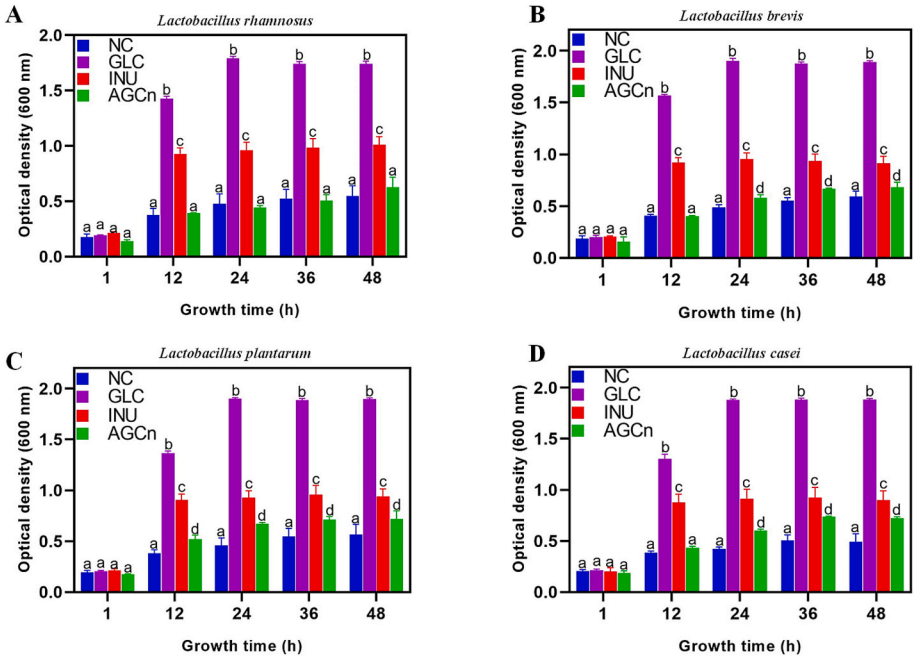


Fig. 3. Growth of strains (A) *Lactobacillus rhamnosus*, (B) *Lactobacillus brevis*, (C) *Lactobacillus plantarum* and (D) *Lactobacillus casei* in MRS broth without glucose: distilled water, Negative control - NC (blue), Glucose - GLC (purple), Inulin – INU (red) and arabinogalactan extracted from *Cenostigma nordestinum* gum – AGCn (green) as carbon sources. Statistical data were considered significant with $p < 0.05$, where distinct letters indicate significant differences.

showing bacterial growth in the negative control group.

The degree of carbohydrate polymerisation correlates with their suitability as a carbon source for different probiotic strains (Lu et al., 2021). Using AGCn as a carbon source, the growth rate of *L. brevis* and *L. casei* deviated from the NC group after 24 h of fermentation. On the other hand, *L. plantarum* exhibited this difference after 12 h of growth compared to the NC group (Fig. 3).

Prebiotics can facilitate the promotion of beneficial bacterial growth. In addition, the rate at which probiotic microorganisms grow on a specific carbon source will influence their ability to compete with other intestinal bacteria in the colon. Thus, the degree of prebiotic activity of a specific carbohydrate is related to the extent to which the carbohydrate is converted into biomass (Nobre et al., 2018). This may justify that AGCn favored the growth of *L. brevis*, *L. plantarum* and *L. casei*, while *L. rhamnosus* did not utilize AGCn. This provides valuable information to predict the modulation of an appropriate gut microbiota composition (Park et al., 2022). In this study, it was observed that *L. rhamnosus* was unable to utilize AGCn as a carbon source and did not achieve bacterial growth, showing optical density values that were statistically similar to those of the NC group (Fig. 3A). Data on the structural complexity of this polymer, attributed to the monosaccharide composition, type of glycosidic bond and degree of branching, may suggest that *L. rhamnosus* does not possess an enzymatic mechanism capable of hydrolyzing AGCn *in vitro* (Silva et al., 2023). Also, certain oligosaccharides and polysaccharides require prior enzymatic hydrolysis to facilitate their metabolization by the bacterial strains (Wang, Xiao, et al., 2020).

Overall, it was observed that AGCn can be used as a carbon source for *L. brevis*, *L. plantarum*, and *L. casei*, except for *L. rhamnosus*. This finding highlights the species-specific nature of enzymatic machinery among *Lactobacillus* strains. However, when co-cultured with other bacteria, as in the gut microbiota, cross-feeding interactions can occur between the different *Lactobacillus* and their respective substrates (Roupar et al., 2023). This suggests that the metabolic potential of AGCn may be more fully realized in a complex microbial ecosystem, where cooperative degradation pathways contribute to its utilization.

3.3. Fermentability of AGCn by probiotic bacteria

Typically, gut bacteria metabolize polysaccharides to generate SCFAs, leading to a reduction in colonic pH (Chen et al., 2023). Thus, total carbohydrate consumption and pH variation may be good indicators of the AGCn fermentation process. Fig. 4 shows the changes in total carbohydrate levels and pH observed during microbiota fermentations conducted with all tested carbon sources.

The amount of AGCn significantly diminished during the fermentation process. In the initial 12 h of fermentation, its concentration markedly decreased from 935 mg/g to 351 mg/g, accounting for a consumption of 62.45 % of AGCn. Subsequently, at 24 h, the total carbohydrates reached 338 mg/g, while the total AGCn at 48 h amounted to 302 mg/g, reflecting consumptions of 3.70 % and 10.65 %, respectively. These findings suggest that although AGCn was mainly digested in the first fermentation hours, it underwent continuous degradation by the gut microbiota up to 48 h. Previous research has shown that the gut microbiota's ability to metabolize polysaccharides during the first 12 h of fermentation may be influenced by the environmental conditions that favor increased bacterial enzymatic activity. However, after this initial period, the availability of nutrients and substrates tends to decrease, leading to a slowdown in the rate of polysaccharide degradation (Holscher, 2017; Nobre et al., 2019).

The gut microbiota does not fully degrade polysaccharides due to the structural complexity of these molecules, which include a diverse composition of monosaccharides, high molecular weight, branching, and variety of glycosidic bonds (Huang et al., 2019; Liu, Liu, et al., 2023). These factors hinder the ability of intestinal bacterial enzymes to access the glycosidic bonds within polysaccharides, thereby prolonging the degradation process. In addition, some intestinal bacteria may partially store polysaccharides as an energy source rather than completely degrading them. This behavior contributes to the incomplete fermentation of these carbohydrates in the gut and may explain the residual concentration of non-degraded AGCn observed following microbiota fermentation (Silva et al., 2023; Zhang et al., 2018).

Regarding the pH assessment during fermentation, the pH values of the INU and AGCn fermentations were not statistically different between

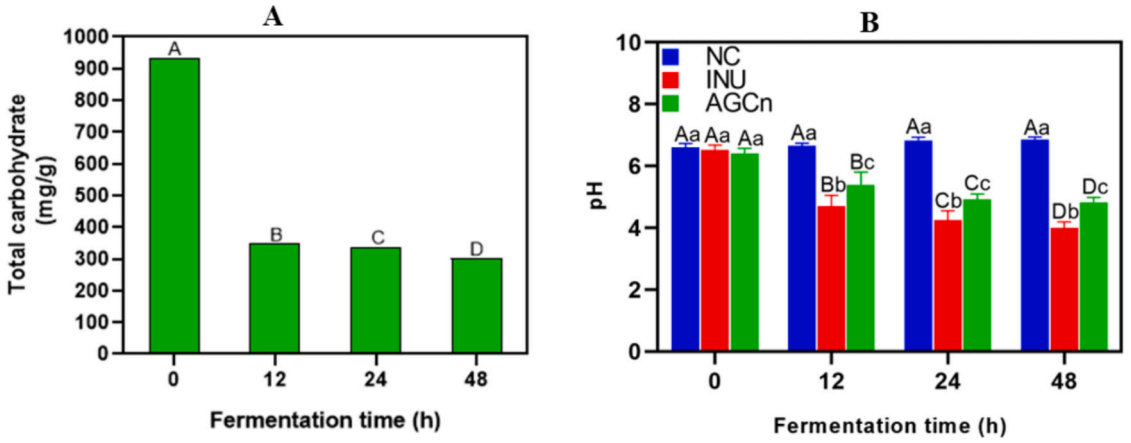


Fig. 4. (A) Profile of the consumption of arabinogalactan extracted from *Cenostigma nordestinum* (AGCn) during the fermentation, and (B) pH values obtained during the fermentation of water as Negative control - NC (blue), inulin – INU (red) and AGCn (green) as carbon sources. Statistical data was considered significant at $p < 0.05$, different letters indicate significant differences between experimental groups across fermentation times (capital letters), and differences between experimental groups at the same time point (lowercase letters).

the two carbohydrates. However, they were statistically different from the NC group. The pH values of the INU and AGCn fermentations gradually decreased over the course of the fermentation, whereas the NC group showed no significant changes throughout the fermentation period.

Nonethless, the results showed that for the same time point, the pH of AGCn decreased less than INU, with a statistically significant difference between the experimental groups (Fig. 4B, lowercase letters). This suggests that AGCn was fermented more slowly than INU. The structure of inulin may explain this slower fermentation rate; as a linear fructose polymer linked by →1)-β-Fru*f*-(2→ bonds, inulin is more readily accessible to bacteria. In contrast, AGCn is fermented more slowly due to its high average molecular weight (8.35×10^4 g/mol) and a more complex monosaccharide composition. On the other hand, this slower fermentation rate might make it available for fermentation in the distal colon, where it could potentially exert beneficial health effects (Liu, Zhao, et al., 2023).

It is also known that lowering the pH in the gut microenvironment can limit or inhibit the growth of pathogenic bacteria and benefit the growth of some beneficial species (Andrade et al., 2020). The AGCn and INU groups induced significant changes in pH values throughout the faecal fermentation process. These changes are possibly related to bacterial diversity, with a reduction in pathogenic bacteria that cannot thrive in relatively acidic pH environments. In addition, these changes may be associated with the production of SCFAs and exert important effects on regulating the intestinal microenvironment (Liu et al., 2024).

During prebiotic metabolism, organic acids such as lactate and short-chain fatty acids (SCFAs) represent the main bacterial end products

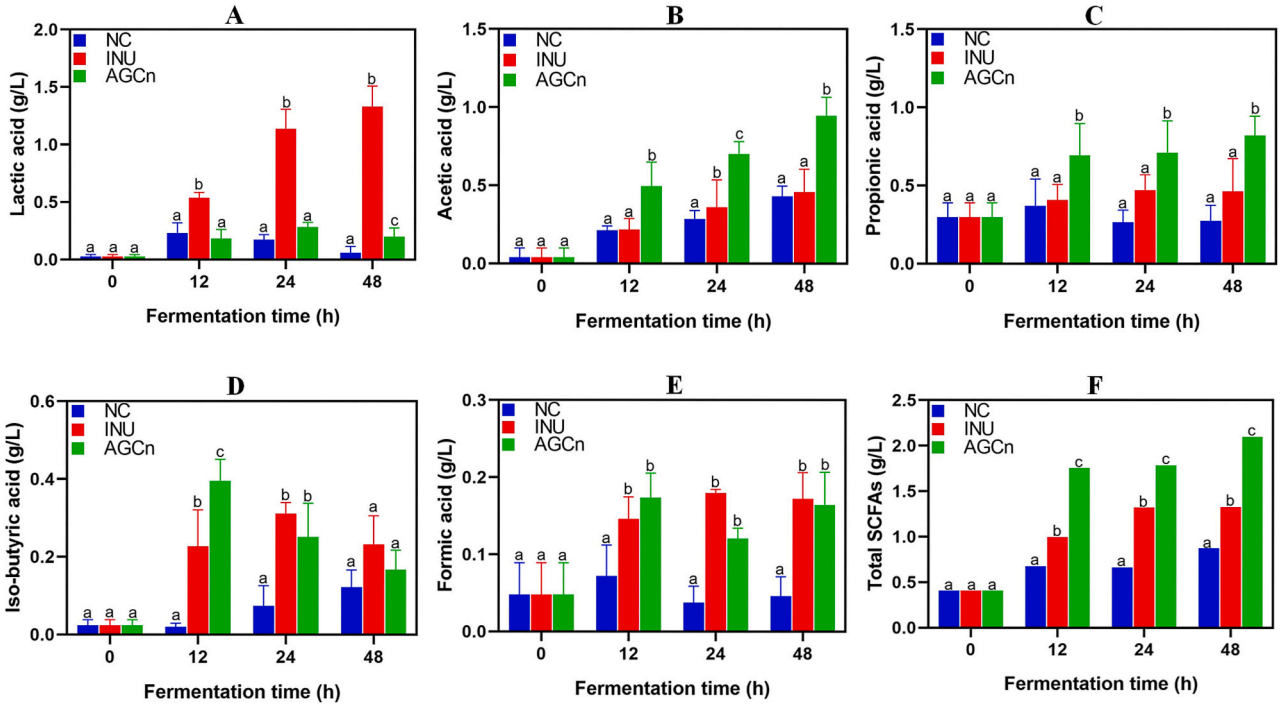


Fig. 5. Concentrations of organic acids, (A) lactic acid, (B) acetic acid, (C) propionic acid, (D) iso-butyric acid, (E) formic acid, and (F) total SCFAs (short-chain fatty acids), produced during the fermentation of arabinogalactan extracted from *Cenostigma nordestinum* – AGCn (green), inulin – INU (red), or water as Negative control - NC (blue). Statistical data were considered significant with $p < 0.05$, where distinct letters indicate significant differences.

(Chen et al., 2020). As observed, the human gut microbiota's fermentation of INU and AGCn resulted in significant levels of lactate, acetate, propionate, iso-butyrate, and formic acid (Fig. 5A–F).

Notably, AGCn promoted the production of acetate, propionate, iso-butyrate, and formic acid at high concentrations, which can be attributed to the bacterial diversity present in the microbiota of the donors. In addition, the INU group exhibited high levels of lactate, which is explained by the ability of lactic acid bacteria to efficiently convert inulin into lactic acid (Sevim et al., 2019). Moreover, the total SCFAs content in the AGCn group increased significantly from 0.40 g/L (0 h) to 2.09 g/L at 48 h. In comparison, the INU group showed lower total SCFAs levels, reaching 1.32 g/L at 48 h, while the NC group presented even lower levels, with 0.87 g/L after 48 h fermentation (Fig. 5F).

Organic acids were produced in all fermentations. The production of organic acids in the NC group could be attributed to protein utilization by proteolytic bacteria (Chen et al., 2023). The results showed that AGCn supplementation produced a diversity of organic acids that decreased pH value, potentially maintaining intestinal homeostasis (Chen et al., 2020). Levels of acetate, butyrate, and propionate were also produced by fermentation of the polysaccharides from gum arabic, tragacanth, and peach (Modrackova et al., 2019; Wei et al., 2022).

At 12 h fermentation, AGCn showed a better effect on the production and richness of acetic acid, propionic acid, iso-butyric acid and total SCFAs than INU, which may be related to the more diverse composition of monosaccharides in AGCn (Liu, Zhao, et al., 2023). The production of formic acid levels in the AGCn group was statistically similar to INU, while lactic acid was produced in highly amount in the INU group.

In the present study, the effect of AGCn on the modulation of gut microbial composition was evaluated by 16S rRNA gene sequencing analysis. Bacterial diversity reflects the abundance of various bacterial species present in the experimental groups (Xiong et al., 2023). The microbial compositions of the initial fermentation time (basal) and after fermentation of inulin (INU) or AGCn were first analyzed at the phylum level, as shown in Fig. 6A. The dominant compositions in the AGCn group were *Actinobacteria* > *Firmicutes* > *Bacteroidetes* while the INU group showed dominance of the *Firmicutes* > *Bacteroidetes* > *Actinobacteria phyla*. The dominant compositions in the basal group showed less bacterial diversity, with *Firmicutes* > *Bacteroidetes* > *Actinobacteria* dominating.

The relative abundance of *Actinobacteria* and *Bacteroidetes* increased by 39.99 ± 11.06 % and 10.28 ± 6.40 %, respectively, after 24 h of fermentation of AGCn. It has been reported that the phyla *Actinobacteria*, *Firmicutes* and *Bacteroidetes* are active in reducing systemic inflammation, improving the recovery rate of tissue structures, increasing the content of SCFAs and restoring the gut microbiota (Liu, Zhao, et al., 2023). The predominance of the phylum *Actinobacteria* in the AGCn group is related to the abundance of *Bifidobacterium*. This indicates the prebiotic potential of AGCn, as *Bifidobacterium* is a very well-known probiotic bacterium (Binda et al., 2018). *Firmicutes* act mainly in the production of acetate during the degradation of carbohydrates, while *Bacteroidetes* use dietary fibers and starch as a source of energy and can act as an important source in the production of propionate (Liu, Zhao, et al., 2023; Wei et al., 2022). In addition, the presence of a large number of carbohydrate-active enzymes (CAZymes) in the phylum *Bacteroidetes* may be responsible for the significant increase in their relative abundance during the AGCn fermentation, as these enzymes play a crucial role in the degradation of highly complex polysaccharides into simpler substrates (Liu et al., 2021; Silva et al., 2023; Wei et al., 2022; Wu et al., 2022).

The distributions of intestinal bacteria at the genus level in the experimental INU and AGCn groups are shown in Fig. 6B. The results showed an elevated relative abundance of *Bifidobacterium* and *Bacteroides* in the AGCn group compared to the initial microbiota (basal). The INU group, on the other hand, exhibited a predominance of *Lactobacillus* and *Bacteroides* at the phylum level. In contrast, the basal group showed an abundance of *Blautia*, *Bacteroides*, and *Ruminococcus* genera. Compared to the basal group, the relative abundance of bacterial genera that are associated with beneficial effects on the host, such as *Bifidobacterium* and *Bacteroides*, increased considerably by 43.81 ± 17.32 % and 7.11 ± 0.40 %, respectively, in the AGCn group. Generally, the genus *Bifidobacterium* is identified as one of the most important probiotics in the human intestine, which can protect against enteropathogenic infections in the host by producing acetate (Wu et al., 2022). As already mentioned, the carbohydrate-degrading enzymes encoded by *Bacteroides* outnumber those encoded by *Firmicutes*, which explains the increase in *Bacteroides* and the low predominance of *Firmicutes* in the AGCn group. A notable example is glycoside hydrolase, which plays a key role in the hydrolysis of non-digestible polysaccharides and

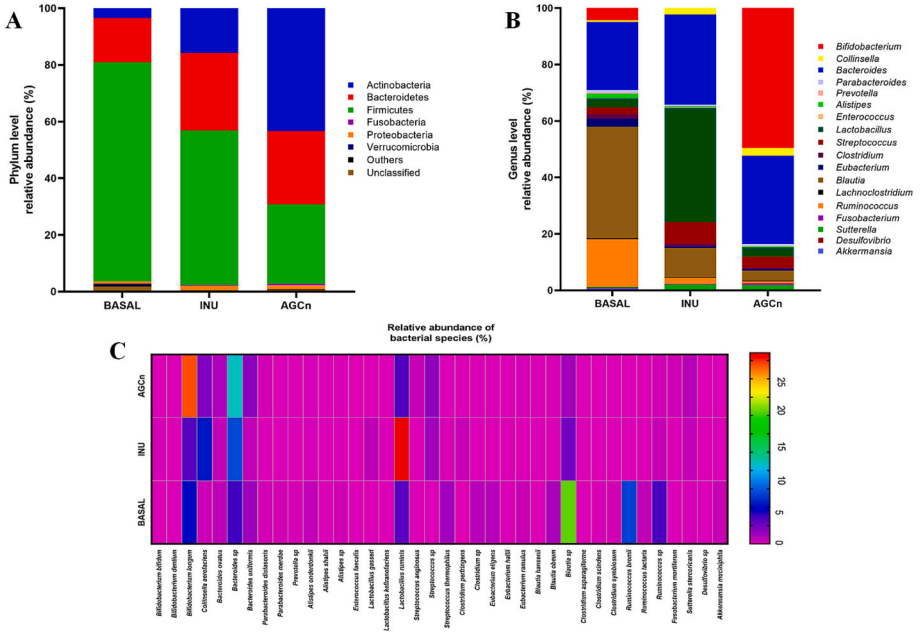


Fig. 6. Relative abundance of the bacterial community at the level of (A) phylum, (B) genus and (C) bacterial species in the gut microbiota before fermentation (BASAL) and after 24 h fermentation with inulin (INU) and arabinogalactan extracted from *Cenostigma nordestinum* gum (AGCn).

stimulates the high production of SCFAs (Liu et al., 2021).

The analysis of bacterial species conducted through 16S rRNA gene sequencing revealed that the AGCn group induced changes in the composition of the gut microbiota (Fig. 6C). AGCn showed an excellent ability to stimulate the growth of *B. longum* and *Bacteroides* sp., which accounted for 48.82 ± 13.36 % and 21.87 ± 12.57 %, respectively, of the total bacterial population (Supplementary material; Table S1). The percentage relative abundance of the most prevalent bacterial species among the experimental groups is shown in Fig. S4 (Supplementary material). It was observed that the high growth of *B. longum* and *Bacteroides sp* in the AGCn group was statistically different from the basal and INU groups. In addition, the INU group significantly favored the growth of *Lactobacillus ruminis*.

The growth of these bacterial species in the AGCn may explain the high production of SCFAs, since *B. longum* and *Bacteroides* sp. are recognized for their ability to use different carbohydrates as an energy source for intestinal epithelial cells, generating the production of acetate, butyrate, and propionate (Rios-Covian et al., 2013; Wang et al., 2021). With an increase in the relative abundance of bacterial species associated with beneficial effects on the host, such as *B. longum* and *Bacteroides* sp. in the AGCn group, a reduction in the relative abundance of Proteobacteria species, commonly associated with intestinal diseases, was observed (Gautério et al., 2022). In addition, the high levels of SCFAs in the INU group can be explained by the growth of L. *ruminis* and *Bacteroides* sp., species with the presence of enzymes capable of fermenting different oligosaccharides (Cheng et al., 2022; Fan et al., 2021). Overall, the AGCn group exerted a prebiotic effect *in vitro*, favoring the growth of beneficial bacteria in the gut microbiota.

4. Conclusion

The structural characterization of the polysaccharide from *C. nordestinum* gum demonstrated that it is an arabinogalactan, structurally constituted by a main chain of the residue →6)-β-Gal*p*-(1→ with branched residues of →3,6)-β-Gal*p*-(1→, →3,4,6)-β-Gal*p*-(1 →, and side chains of residues of 3-α-Ara*f* and 5-α-Ara*f*, with α-Ara*f* and α-Rha*p* as terminally linked residues. The arabinogalactan also contained →4)-α-Gal*p*A-(1→, a moiety of pectic polysaccharide. Among these structural characteristics, the →3,4,6)-β-Gal*p*-(1→ residue stands out, which, to date, has not been reported in plant exudates. Its fermentation by healthy microbiota reduced faecal pH and high production of endogenous levels of organic acids (lactate and SCFAs). Furthermore, there was a significant increase in the abundance of bacteria beneficial to the host's health, such as *Bifidobacterium longum* and *Bacteroides* sp. This demonstrates that AGCn has prebiotic potential, capable of altering the composition of the gut microbiota and promoting the production of beneficial metabolites that can improve intestinal health. Therefore, AGCn may represent a potential application in the food industry as a natural functional component and in therapies for reversing dysbiosis.

CRediT authorship contribution statement

Francisca Crislândia Oliveira Silva: Writing – original draft, Methodology, Investigation, Formal analysis, Data curation, Conceptualization. **Maria Isabela Ferreira de Araújo:** Methodology, Formal analysis, Data curation. **Soraia P. Silva:** Methodology, Formal analysis, Data curation. **Elisabete Coelho:** Writing – review & editing, Methodology, Formal analysis, Data curation. **Aline Teixeira dos Santos:** Methodology, Formal analysis, Data curation. **Abigail González:** Methodology, Formal analysis, Data curation. **Andreia Filipa Ferreira Salvador:** Methodology, Formal analysis, Data curation. **Thiago Barbosa Cahú:** Visualization, Methodology, Investigation, Data curation, Conceptualization. **Angélica Thomaz Vieira:** Visualization, Data curation, Conceptualization. **Marthyna Pessoa de Souza:** Formal analysis, Data curation. **Manuel A. Coimbra:** Writing – review & editing, Visualization, Conceptualization. **José A. Teixeira:** Visualization, Conceptualization. **Clarisse Nobre:** Writing – review & editing, Visualization, Supervision, Methodology, Investigation, Funding acquisition, Data curation, Conceptualization. **Paulo Antônio Galindo Soares:** Writing – review & editing, Writing – original draft, Visualization, Validation, Supervision, Methodology, Investigation, Funding acquisition, Data curation, Conceptualization. **Maria Tereza dos Santos Correia:** Visualization, Validation, Supervision, Funding acquisition.

Declaration of competing interest

The authors declare that they have no known competing financial interests or personal relationships that could have appeared to influence the work reported in this paper.

Acknowledgements

The authors express their gratitude to the Conselho Nacional de Desenvolvimento Científico e Tecnológico (CNPq) and Fundação de Amparo à Ciência e Tecnologia de Pernambuco (FACEPE) (Process: 0546-2.08/20) for the research grants and financial support. This work was supported by the Federal University of Pernambuco and partly funded by the CNPq (Process: 400585/2022-7). It was also supported by the Portuguese Foundation for Science and Technology (FCT) under the scope of the strategic funding of UIDB/04469 unit, by LABBELS – Associate Laboratory in Biotechnology, Bioengineering and Microelectromechanical Systems, LA/P/0029/2020 and by LAQV/REQUIMTE unit [LA/P/0008/2020 DOI 10.54499/LA/P/0008/2020, UIDP/50006/2020 DOI 10.54499/UIDP/50006/2020 and UIDB/50006/2020 DOI 10.54499/UIDB/50006/2020] through national funds and ERDF, within the PT2020 Partnership Agreement. Abigail González and E. Coelho acknowledge the FCT for the PhD Grant 2021.06268.BD, and for the Assistant Research Contract (2023.08855.CEECIND), respectively.

Appendix A. Supplementary data

Supplementary data to this article can be found online at https://doi.org/10.1016/j.carbpol.2025.123738.

Data availability

Data will be made available on request.

References

Adak, A., & Khan, M. R. (2019). An insight into gut microbiota and its functionalities. *Cellular and Molecular Life Sciences, 76*(3), 473–493. https://doi.org/10.1007/s00018-018-2943-4

Ahmadi, E., Rezadoost, H., Alilou, M., Stuppner, H., & Moridi Farimani, M. (2022). Purification, structural characterization and antioxidant activity of a new arabinogalactan from *Dorema ammoniacum* gum. *International Journal of Biological Macromolecules, 194*, 1019–1028. https://doi.org/10.1016/j.ijbiomac.2021.11.163

Andrade, A. C., Marinho, J. F. U., de Souza, A. C., de Sousa Tavares, T., Dias, D. R., Schwan, R. F., … Bastos, S. C. (2020). Prebiotic potential of pulp and kernel cake from Jerivá (*Syagrus romanzoffiana*) and Macaúba palm fruits (*Acrocomia aculeata*). *Food Research International, 136*, Article 109595. https://doi.org/10.1016/j.foodres.2020.109595

Bamigbade, G. B., Subhash, A. J., Kamal-Eldin, A., Nyström, L., & Ayyash, M. (2022). An updated review on prebiotics: Insights on potentials of food seeds waste as source of potential prebiotics. *Molecules, 27*(18), 5947. https://doi.org/10.3390/molecules27185947

Bastos, R., Coelho, E., & Coimbra, M. A. (2015). Modifications of *Saccharomyces pastorianus* cell wall polysaccharides with brewing process. *Carbohydrate Polymers, 124*, 322–330. https://doi.org/10.1016/j.carbpol.2015.02.031

Bhushette, P. R., & Annapure, U. S. (2018). Physicochemical, functional and rheological investigation of *Soymida febrifuga* exudate gum. *International Journal of Biological Macromolecules, 111*, 1116–1123. https://doi.org/10.1016/j.ijbiomac.2018.01.117

Binda, C., Lopetuso, L. R., Rizzatti, G., Gibiino, G., Cennamo, V., & Gasbarrini, A. (2018). Actinobacteria: A relevant minority for the maintenance of gut homeostasis. *Digestive and Liver Disease, 50*(5), 421–428. https://doi.org/10.1016/j.dld.2018.02.012

Bradford, M. M. (1976). Interactive effects of drought stress and chitosan application on physiological characteristics and essential oil yield of *Thymus daenensis* Celak. *Crop Journal, 5*(5), 407–415. https://doi.org/10.1016/j.cj.2017.04.003

Chaudhari, B. B., & Annapure, U. S. (2020). Physiochemical and rheological characterization of *Pithecellobium dulce* (Roxb.) benth gum exudate as a potential wall material for the encapsulation of rosemary oil. *Carbohydrate Polymer Technologies and Applications, 1*, Article 100005. https://doi.org/10.1016/j.carpta.2020.100005

Chaudhari, B. B., & Annapure, U. S. (2021). Rheological, physicochemical, and spectroscopic characterizations of *Limonia acidissima* L. gum exudate with an application in extrusion processing. *Carbohydrate Polymer Technologies and Applications, 2*, Article 100020. https://doi.org/10.1016/j.carpta.2020.100020

Chen, G.-j., Hong, Q.-y., Ji, N., Wu, W.-n., & Ma, L.-z. (2020). Influences of different drying methods on the structural characteristics and prebiotic activity of polysaccharides from bamboo shoot (*Chimonobambusa quadrangularis*) residues. *International Journal of Biological Macromolecules, 155*, 674–684. https://doi.org/10.1016/j.ijbiomac.2020.03.223

Chen, S., Luan, L., Zhang, Y., Liu, F., Ye, X., & Hou, Z. (2023). A comparison study on polysaccharides extracted from *Rosa sterilis* S.D. Shi using different methods: Structural and in vitro fermentation characterizations. *Food Chemistry, 17*, Article 100533. https://doi.org/10.1016/j.fochx.2022.100533

Cheng, J., Hu, J., Geng, F., & Nie, S. (2022). Bacteroides utilization for dietary polysaccharides and their beneficial effects on gut health. *Food Science and Human Wellness, 11*(5), 1101–1110. https://doi.org/10.1016/j.fshw.2022.04.002

Cheng, K., Zhou, Y., & Neelamegham, S. (2017). DrawGlycan-SNFG: A robust tool to render glycans and glycopeptides with fragmentation information. *Glycobiology, 27*, 200–205. https://doi.org/10.1093/glycob/cww115

Coelho, M. N., Soares, P. A. G., Frattani, F. S., Camargo, L. M. M., Tovar, A. M. F., de Aguiar, P. F., … Costa, S. S. (2020). Polysaccharide composition of an anticoagulant fraction from the aqueous extract of *Marsypianthes chamaedrys* (Lamiaceae). *International Journal of Biological Macromolecules, 145*, 668–681. https://doi.org/10.1016/j.ijbiomac.2019.12.176

De, A., Malpani, D., Das, B., Mitra, D., & Samanta, A. (2020). Characterization of an arabinogalactan isolated from gum exudate of *Odina wodier* Roxb.: Rheology, AFM, Raman and CD spectroscopy. *Carbohydrate Polymers, 250*, Article 116950. https://doi.org/10.1016/j.carbpol.2020.116950

de Araujo, D. F., Madeira, J.d. C., Cunha, A. P., Ricardo, N. M. P. S., Bezerra, F. F., Mourão, P. A. S., … Pereira, M. G. (2021). Structural characterization of anticoagulant and antithrombotic polysaccharides isolated from *Caesalpinia ferrea* stem barks. *International Journal of Biological Macromolecules, 175*, 147–155. https://doi.org/10.1016/j.ijbiomac.2021.01.177

de Sousa, L. M. S., Santos, B. N. G., Medeiros, M.d. G. F., Lima, I. B. C., Santos-Filho, F. S., Santana, A. C. S. G. V., … Nunes, L. C. C. (2021). *Poincianella pyramidalis* (Tul) L.P. Queiroz: A review on traditional uses, phytochemistry and biological-pharmacological activities. *Journal of Ethnopharmacology, 264*, 113–181. https://doi.org/10.1016/j.jep.2020.113181

Elshahed, M. S., Miron, A., Aprotosoaie, A. C., & Farag, M. A. (2021). Pectin in diet: Interactions with the human microbiome, role in gut homeostasis, and nutrient-drug interactions. *Carbohydrate Polymers, 255*, Article 117388. https://doi.org/10.1016/j.carbpol.2020.117388

Enam, F., & Mansell, T. J. (2019). Prebiotics: Tools to manipulate the gut microbiome and metabolome. *Journal of Industrial Microbiology & Biotechnology, 46*(10), 1445–1459. https://doi.org/10.1007/s10295-019-02203-4

Eshun Oppong, E., Kuntworbe, N., Asantewaa Osei, Y., Ofori-Kwakye, K., Adi-Darko, O., & Obese, E. (2021). Physicochemical characterisation of *Piptadeniastrum africana* (hook. F.) gum, a potential pharmaceutical excipient. *Scientific African, 13*, Article e00925. https://doi.org/10.1016/j.sciaf.2021.e00925

Fan, X., Bai, Y., Fan, T. P., Zheng, X., & Cai, Y. (2021). A single point mutation engineering for changing the substrate specificity of D-lactate dehydrogenase from *Lactobacillus fermentum. LWT, 151*. https://doi.org/10.1016/j.lwt.2021.112209

Fu, Y. P., Li, C. Y., Peng, X., Zou, Y. F., Rise, F., Paulsen, B. S., … Inngjerdingen, K. T. (2022). Polysaccharides from *Aconitum carmichaelii* leaves: Structure, immunomodulatory and anti-inflammatory activities. *Carbohydrate Polymers, 291*, Article 119655. https://doi.org/10.1016/j.carbpol.2022.119655

Gautério, V. G., Amorim, C., Silvério, S. C., Cardoso, B. B., Ballesteros, L. F., Alves, J. I., … Rodrigues, L. R. (2022). Hydrolysates containing xylooligosaccharides produced by different strategies: Structural characterization, antioxidant and prebiotic activities. *Food Chemistry, 391*. https://doi.org/10.1016/j.foodchem.2022.133231

Gavlighi, H. A., Meyer, A. S., Zaidel, D. N. A., Mohammadifar, M. A., & Mikkelsen, J. D. (2013). Stabilization of emulsions by gum tragacanth (*Astragalus* spp.) correlates to the galacturonic acid content and methoxylation degree of the gum. *Food Hydrocolloids, 31*(1), 5–14. https://doi.org/10.1016/j.foodhyd.2012.09.004

Gibson, G. R., Hutkins, R., Sanders, M. E., Prescott, S. L., Reimer, R. A., Salminen, S. J., … Reid, G. (2017). Expert consensus document: The International Scientific Association for Probiotics and Prebiotics (ISAPP) consensus statement on the definition and scope of prebiotics. *Nature Reviews Gastroenterology and Hepatology, 14*(8), 491–502. https://doi.org/10.1038/nrgastro.2017.75

Gudiña, E. J., Couto, M. R., Silva, S. P., Coelho, E., Coimbra, M. A., Teixeira, J. A., & Rodrigues, L. R. (2023). Sustainable exopolysaccharide production by *Rhizobium viscosum* CECT908 using corn steep liquor and sugarcane molasses as sole substrates. *Polymers, 15*(1), 20. https://doi.org/10.3390/polym15010020

Hamed, M., Coelho, E., Bastos, R., Evtuguin, D. V., Ferreira, S. S., Lima, T., … Bougatef, A. (2022). Isolation and identification of an arabinogalactan extracted from Pistachio external hull: Assessment of immunostimulatory activity. *Food Chemistry, 373*, Article 131416. https://doi.org/10.1016/j.foodchem.2021.131416

Holscher, H. D. (2017). Dietary fiber and prebiotics and the gastrointestinal microbiota. *Gut Microbes, 8*(2), 172–184. https://doi.org/10.1080/19490976.2017.1290756

Hooks, K. B., & O'Malley, M. A. (2017). Dysbiosis and its discontents. *mBio, 8*(5), 1–11. https://doi.org/10.1128/mBio.01492-17

Huang, F., Hong, R., Zhang, R., Dong, L., Bai, Y., Liu, L., Jia, X., Wang, G., & Zhang, M. (2019). Dynamic variation in biochemical properties and prebiotic activities of polysaccharides from longan pulp during fermentation process. *International Journal of Biological Macromolecules, 132*, 915–921. https://doi.org/10.1016/j.ijbiomac.2019.04.032

K-da, S., Peerakietkhajorn, S., Siringoringo, B., Muangnil, P., Wichienchot, S., & Khuituan, P. (2020). Oligosaccharides from *Gracilaria fisheri* ameliorate gastrointestinal dysmotility and gut dysbiosis in colitis mice. *Journal of Functional Foods, 71*, Article 104021. https://doi.org/10.1016/j.jff.2020.104021

Kheradkhord, A., & Shekarchizadeh, H. (2022). Structural, physicochemical and functional properties of an exudate gum: Opopanax gum. *Journal of Food Measurement and Characterization, 16*(3), 2201–2210. https://doi.org/10.1007/s11694-022-01330-4

Lakhera, A. K., & Kumar, V. (2017). Monosaccharide composition of acidic gum exudates from Indian *Acacia tortilis* ssp. raddiana (Savi) Brenan. *International Journal of Biological Macromolecules, 94*, 45–50. https://doi.org/10.1016/j.ijbiomac.2016.09.097

Li, H., Xie, W., Qiao, X., Cui, H., Yang, X., & Xue, C. (2020). Structural characterization of arabinogalactan extracted from *Ixeris chinensis* (Thunb.) Nakai and its immunomodulatory effect on RAW264.7 macrophages. *International Journal of Biological Macromolecules, 143*, 977–983. https://doi.org/10.1016/j.ijbiomac.2019.09.158

Li, N., Yang, F., Su, J., Shi, S., Ordaz-Ortiz, J. J., Cheng, X., Xiong, S., Xu, Y., Wu, J., Wang, H., & Wang, S. (2022). Structure characterization of an arabinogalactan from *Cynanchum atratum* and its immune stimulatory activity on RAW264.7 cells. *International Journal of Biological Macromolecules, 194*, 163–171. https://doi.org/10.1016/j.ijbiomac.2021.11.172

Lima, L. R. M., Ramos, E. L.d. L., Silva, M. F. S., Ribeiro, F.d. O. S., Sousa, J. S., Pessoa, C., … de Paula, R. C. M. (2021). Poly(N-isopropylacrylamide)/galactomannan from *Delonix regia* seed thermal responsive graft copolymer via schiff base reaction. *International Journal of Biological Macromolecules, 166*, 144–154. https://doi.org/10.1016/j.ijbiomac.2020.10.121

Liu, C., Du, P., Guo, Y., Xie, Y., Yu, H., Yao, W., Cheng, Y., & Qian, H. (2021). Extraction, characterization of aloe polysaccharides and the in-depth analysis of its prebiotic effects on mice gut microbiota. *Carbohydrate Polymers, 261*, Article 117874. https://doi.org/10.1016/j.carbpol.2021.117874

Liu, M., Liu, X., Bi, J., Lyu, J., Wu, X., Zhou, M., & Liu, J. (2023). Comparative study on physicochemical properties of thirteen peach gums from different varieties. *Scientia Horticulturae, 310*, Article 111722. https://doi.org/10.1016/j.scienta.2022.111722

Liu, T., Zhao, M., Zhang, Y., Wang, Z., Yuan, B., Zhao, C., & Wang, M. (2023). Integrated microbiota and metabolite profiling analysis of prebiotic characteristics of *Phellinus linteus* polysaccharide in vitro fermentation. *International Journal of Biological Macromolecules, 242*. https://doi.org/10.1016/j.ijbiomac.2023.124854

Liu, X., Su, S., Yao, J., Zhang, X., Wu, Z., Jia, L., Liu, L., Hou, Y., Faragb, M., & Liu, L. (2024). Research advance about plant polysaccharide prebiotics, benefit for probiotics on gut homeostasis modulation. *Food Bioscience, 59*, 103831. https://doi.org/10.1016/j.fbio.2024.103831

Lu, X., Li, N., Zhao, R., Zhao, M., Cui, X., Xu, Y., & Qiao, X. (2021). In vitro prebiotic properties of garlic polysaccharides and its oligosaccharide mixtures obtained by acid hydrolysis. *Frontiers in Nutrition, 9*(8), Article 798450. https://doi.org/10.3389/fnut.2021.798450

Mauri, L., Boccardi, G., Torri, G., Karfunkle, M., Macchi, E., Muzi, L., Keire, D., & Guerrini, M. (2017). Qualification of HSQC methods for quantitative composition of heparin and low molecular weight heparins. *Journal of Pharmaceutical and Biomedical Analysis, 136*, 92–105. https://doi.org/10.1016/j.jpba.2016.12.031

Melo, A. M. A., Oliveira, M. R. F., Furtado, R. F., de Fatima Borges, M., Biswas, A., Cheng, H. N., & Alves, C. R. (2020). Preparation and characterization of carboxymethyl cashew gum grafted with immobilized antibody for potential biosensor application. *Carbohydrate Polymers, 228*, Article 115408. https://doi.org/10.1016/j.carbpol.2019.115408

Mitra, D., Sikdar, S., Chakraborty, M., Das, O., Samanta, A., & Dutta, S. (2023). Gum Odina prebiotic prevents experimental colitis in C57BL/6 mice model and its role in shaping gut microbial diversity. *Food Bioscience, 53*, Article 102509. https://doi.org/10.1016/j.fbio.2023.102509

Modrackova, N., Makovska, M., Mekadim, C., Vlkova, E., Tejnecky, V., Bolechova, P., & Bunesova, V. (2019). Prebiotic potential of natural gums and starch for bifidobacteria of variable origins. *Bioactive Carbohydrates and Dietary Fibre, 20*, Article 100199. https://doi.org/10.1016/j.bcdf.2019.100199

Munteanu, C., & Schwartz, B. (2024). Interactions between dietary antioxidants, dietary fiber and the gut microbiome: Their putative role in inflammation and cancer. *International Journal of Molecular Sciences, 25*(15), 8250. https://doi.org/10.3390/ijms25158250

Mutuyemungu, E., Singh, M., Liu, S., & Rose, D. J. (2023). Intestinal gas production by the gut microbiota: A review. *Journal of Functional Foods, 100*, Article 105367. https://doi.org/10.1016/j.jff.2022.105367

NeuHannig, C., Régis, C.d. P., Soika, J. H., Silva, L. A.d. S., Quintanilha, V. A. B., Bussolotto, L. T., … Bello, S. R. B. (2019). Intestinal dysbiosis: Correlation with current chronic diseases and nutritional intervention. *Research, Society and Development, 8*(6), 1–7. https://doi.org/10.33448/rsd-v8i6.1054

Nobre, C., do Nascimento, A. K. C., Silva, S. P., Coelho, E., Coimbra, M. A., Cavalcanti, M. T. H., … Porto, A. L. F. (2019). Process development for the production of prebiotic fructo-oligosaccharides by *Penicillium citreonigrum*.

Bioresource Technology, 282, 464–474. https://doi.org/10.1016/j.biortech.2019.03.053

Nobre, C., Simões, L. S., Gonçalves, D. A., Berni, P., & Teixeira, J. A. (2022). *5 - Fructooligosaccharides production and the health benefits of prebiotics*. https://doi.org/10.1016/B978-0-12-823506-5.00002-3

Nobre, C., Sousa, S. C., Silva, S. P., Pinheiro, A. C., Coelho, E., Vicente, A. A., … Rodrigues, L. R. (2018). In vitro digestibility and fermentability of fructo-oligosaccharides produced by *Aspergillus ibericus*. *Journal of Functional Foods, 46*, 278–287. https://doi.org/10.1016/j.jff.2018.05.004

Nunes, F. M., Reis, A., Silva, A. M. S., Domingues, M. R. M., & Coimbra, M. A. (2008). Rhamnoarabinosyl and rhamnoarabinoarabinosyl side chains as structural features of coffee arabinogalactans. *Phytochemistry, 69*(7), 1573–1585. https://doi.org/10.1016/j.phytochem.2008.01.021

Park, S., Saravanakumar, K., Sathiyaseelan, A., Han, K. S., Lee, J., & Wang, M. H. (2022). Polysaccharides of *Weissella cibaria* act as a prebiotic to enhance the probiotic potential of *Lactobacillus rhamnosus*. *Applied Biochemistry and Biotechnology, 195*(6), 3928–3940. https://doi.org/10.1007/s12010-022-04104-2

Pereira, L. C. J., Nascimento, F. G., Oliveira, S. R. B. D., Lima, G. C., Chagas, F. D. S., Sombra, V. G., … Freitas, A. L. P. (2021). Protective effect against gastric mucosa injury of a sulfated agaran from *Acanthophora spicifera*. *Carbohydrate Polymers, 261*, Article 117829. https://doi.org/10.1016/j.carbpol.2021.117829

Portincasa, P., Bonfrate, L., Vacca, M., De Angelis, M., Farella, I., Lanza, E., … Di Ciaula, A. (2022). Gut microbiota and short chain fatty acids: Implications in glucose homeostasis. *International Journal of Molecular Sciences, 23*(3), 1105. https://doi.org/10.3390/ijms23031105

Rios-Covian, D., Arboleya, S., Hernandez-Barranco, A. M., Alvarez-Buylla, J. R., Ruas-Madiedo, P., Gueimonde, M., & De Los Reyes-Gavilan, C. G. (2013). Interactions between *Bifidobacterium* and *Bacteroides* species in cofermentations are affected by carbon sources, including exopolysaccharides produced by bifidobacteria. *Applied and Environmental Microbiology, 79*(23), 7518–7524. https://doi.org/10.1128/AEM.02545-13

Rodrigues, E. M., Queiroz, R. T., Silva, L. P., Monteiro, F. K.d. S., & Melo, J. I. M.d. (2020). Fabaceae in a rocky outcrop in the brazilian semiarid. *Rodriguésia, 71*, Article e02252018. https://doi.org/10.1590/2175-7860202071025

Roupar, D., Coelho, M. C., Gonçalves, D. A., Silva, S. P., Coelho, E., Silva, S., … Nobre, C. (2022). Evaluation of microbial-fructo-oligosaccharides metabolism by human gut microbiota fermentation as compared to commercial inulin-derived oligosaccharides. *Foods, 11*(7), 954. https://doi.org/10.3390/foods11070954

Roupar, D., González, A., Martins, J. T., Gonçalves, D. A., Teixeira, J. A., Botelho, C., & Nobre, C. (2023). Modulation of designed gut bacterial communities by prebiotics and the impact of their metabolites on intestinal cells. *Foods, 12*(23), Article 4216. https://doi.org/10.3390/foods12234216

Rymovicz, A. U. M., Souza, R. D., Gursky, L. C., Rosa, R. T., Trevilatto, P. C., Groppo, F. C., & Rosa, E. A. R. (2011). Screening of reducing agents for anaerobic growth of *Candida albicans* SC5314. *Journal of Microbiological Methods, 84*(3), 461–466. https://doi.org/10.1016/j.mimet.2011.01.020

Sevim, S., Topal, G. G., Tengilimoglu-Metin, M. M., Sancak, B., & Kizil, M. (2019). Effects of inulin and lactic acid bacteria strains on aflatoxin M1 detoxification in yoghurt. *Food Control, 100*, 235–239. https://doi.org/10.1016/j.foodcont.2019.01.028

Sharma, A., Bhushette, & Annapure, U. S. (2021). Physicochemical and rheological properties of *acacia catechu* exudate gum. *Carbohydrate Polymer Technologies and Applications, 2*, Article 100127. https://doi.org/10.1016/j.carpta.2021.100127

Sharma, A., Bhushette, P. R., & Annapure, U. S. (2020). Purification and physicochemical characterization of *Prunus domestica* exudate gum polysaccharide. *Carbohydrate Polymer Technologies and Applications, 1*, Article 100003. https://doi.org/10.1016/j.carpta.2020.100003

Silva, F. C. O., Malaisamy, A., Cahú, T. B., Araújo, M. I. F., Soares, P. A. G., Vieira, A. T., & Correia, M. T.d. S. (2023). Polysaccharides from exudate gums of plants and interactions with the intestinal microbiota: A review of vegetal biopolymers and prediction of their prebiotic potential. *International Journal of Biological Macromolecules, 254*, 127715. https://doi.org/10.1016/j.ijbiomac.2023.127715

Singleton, V. L., & Rossi, J. A., Jr. (1965). Colorimetry to total phenolics with phosphomolybdic acid reagents. *American Journal of Enology and Viniculture, 16*(48), 144–158. https://doi.org/10.5344/ajev.1965.16.3.144

Soares, J. M. A., da Silva Júnior, E. D., Oliveira de Veras, B., Yara, R., de Albuquerque, P. B. S., & de Souza, M. P. (2022). Active biodegradable film based on chitosan and *Cenostigma nordestinum*' extracts for use in the food industry. *Journal of Polymers and the Environment, 30*(1), 217–231. https://doi.org/10.1007/s10924-021-02192-5

Soares, P. A. G., Ribeiro, K. A., Valente, A. P., Capillé, N. V., Oliveira, S. N. M. C. G., Tovar, A. M. F., … Mourão, P. A. S. (2018). A unique fucosylated chondroitin sulfate type II with strikingly homogeneous and neatly distributed α-fucose branches. *Glycobiology, 28*(8), 565–579. https://doi.org/10.1093/glycob/cwy048

Sori, N., Poyil, N. C., & Khan, M. (2023). In vitro fermentation of kodo and kutki millets by human gut microbiota: Gut microbiota and metabolomic analysis. *Food Bioscience, 53*, Article 103343. https://doi.org/10.1016/j.fbio.2023.103343

Souza, M. P., Cerqueira, M. A., Souza, B. W. S., Teixeira, J. A., Porto, A. L. F., Vicente, A. A., & Carneiro-da-Cunha, M. G. (2010). Polysaccharide from *Anacardium occidentale* L. tree gum (Policaju) as a coating for Tommy Atkins mangoes. *Chemical Papers, 64*(4), 475–481. https://doi.org/10.2478/s11696-010-0017-7

Speciale, I., Notaro, A., Garcia-Vello, P., Di Lorenzo, F., Armiento, S., Molinaro, A., … De Castro, C. (2022). Liquid-state NMR spectroscopy for complex carbohydrate structural analysis: A hitchhiker's guide. *Carbohydrate Polymers, 277*. https://doi.org/10.1016/j.carbpol.2021.118885

Tai, Y., Shen, J., Luo, Y., Qu, H., & Gong, X. (2020). Research progress on the ethanol precipitation process of traditional Chinese medicine. *Chinese Medicine (United Kingdom), 15*(84), 84. https://doi.org/10.1186/s13020-020-00366-2

Talapko, J., Včev, A., Meštrović, T., Pustijanac, E., Jukić, M., & Škrlec, I. (2022). Homeostasis and dysbiosis of the intestinal microbiota: Comparing hallmarks of a healthy state with changes in inflammatory bowel disease. *Microorganisms, 10*(12), 1–17. https://doi.org/10.3390/microorganisms10122405

Tan, L., Qiu, F., Lamport, D. T. A., & Kieliszewski, M. J. (2004). Structure of a hydroxyproline (Hyp)-arabinogalactan polysaccharide from repetitive Ala-Hyp expressed in transgenic *Nicotiana tabacum*. *The Journal of Biological Chemistry, 279* (13), 13156–13165. https://doi.org/10.1074/jbc.M311864200

Thanzami, K., Malsawmtluangi, C., Lalhlenmawia, H., Seelan, T. V., Palanisamy, S., Kandasamy, R., & Pachuau, L. (2015). Characterization and in vitro antioxidant activity of *Albizia stipulata* Boiv. gum exudates. *International Journal of Biological Macromolecules, 80*, 231–239. https://doi.org/10.1016/j.ijbiomac.2015.06.043

Trabelsi, L., M'sakni, N. H., Ouada, H. B., Bacha, H., & Roudesli, S. (2009). Partial characterization of extracellular polysaccharides produced by cyanobacterium *Arthrospira platensis*. *Biotechnology and Bioprocess Engineering, 14*(1), 27–31. https://doi.org/10.1007/s12257-008-0102-8

Vasile, F. E., Romero, A. M., Judis, M. A., Mattalloni, M., Virgolini, M. B., & Mazzobre, M. F. (2019). Phenolics composition, antioxidant properties and toxicological assessment of *Prosopis alba* exudate gum. *Food Chemistry, 285*, 369–379. https://doi.org/10.1016/j.foodchem.2019.02.003

Wang, A., Du, Q., Li, X., Cui, Y., Luo, J., Li, C., Peng, C., Zhong, X., & Huang, G. (2024). Intracellular and extracellular metabolic response of the lactic acid *Bacterium Weissella confusa* under salt stress. *Metabolites, 14*(12). https://doi.org/10.3390/metabo14120695

Wang, N., Li, Q., Liu, M., Liu, M., & Zhao, Z. (2023). Structural characterization of alkali-extracted jujube polysaccharides and their effects on the fecal microbiota in vitro. *LWT, 184*, Article 115087. https://doi.org/10.1016/j.lwt.2023.115087

Wang, S., Pan, J., Zhang, Z., & Yan, X. (2020). Investigation of dietary fructooligosaccharides from different production methods: Interpreting the impact of compositions on probiotic metabolism and growth. *Journal of Functional Foods, 69*. https://doi.org/10.1016/j.jff.2020.103955

Wang, S., Xiao, Y., Tian, F., Zhao, J., Zhang, H., Zhai, Q., & Chen, W. (2020). Rational use of prebiotics for gut microbiota alterations: Specific bacterial phylotypes and related mechanisms. *Journal of Functional Foods, 66*, Article 103838. https://doi.org/10.1016/j.jff.2020.103838

Wang, Y., Liu, Y., Polic, I. I., Matheyambath, A. C., & LaPointe, G. (2021). Modulation of human gut microbiota composition and metabolites by arabinogalactan and *Bifidobacterium longum* subsp. longum BB536 in the simulator of the human intestinal microbial ecosystem (SHIME®). *Journal of Functional Foods, 87*, Article 104820. https://doi.org/10.1016/j.jff.2021.104820

Wei, C., Yao, L., Zhang, L., Zhang, Y., Luo, Q., Qiu, S., Zeng, X., Chen, S., & Ye, X. (2022). In vitro digestion and fecal fermentation of peach gum polysaccharides with different molecular weights and their impacts on gut microbiota. *Foods, 11*(24). https://doi.org/10.3390/foods11243970

Wei, C., Yao, L., Zhang, Y., Qiu, S., Zeng, X., Chen, S., & Ye, X. (2023). Structural characterization of peach gum polysaccharide and its effects on the regulation of DSS-induced acute colitis. *International Journal of Biological Macromolecules, 225*, 1224–1234. https://doi.org/10.1016/j.ijbiomac.2022.11.183

Wu, Feng, K. L., Li, F., Hu, Y. C., Wang, S. P., Gan, R. Y., & Zou, L. (2022). In vitro digestive characteristics and microbial degradation of polysaccharides from lotus leaves and related effects on the modulation of intestinal microbiota. *Current Research in Food Science, 5*, 752–762. https://doi.org/10.1016/j.crfs.2022.04.004

Wu, J., Xu, Y., Zhu, B., Liu, K., Wang, S., Sheng, Y., Wang, H., Shi, S., Zhang, Q., Wang, S., & Qin, L. (2020). Characterization of an arabinogalactan from the fruit hulls of *Ficus pumila* Linn. and its immunomodulatory effect. *Journal of Functional Foods, 73*. https://doi.org/10.1016/j.jff.2020.104091

Xiong, J., Yu, J., Liu, D., Wu, J.-J., Liang, M.-H., Tang, J., & Xu, Y.-Q. (2023). A polysaccharide from yogurt fermented by *Lactobacillus bulgaricus* and *Streptococcus thermophilus*: Structural characteristics and its alleviative effect on DSS-induced colitis in mice. *Journal of Functional Foods, 109*, Article 105778. https://doi.org/10.1016/j.jff.2023.105778

Yao, H. Y. Y., Wang, J. Q., Yin, J. Y., Nie, S. P., & Xie, M. Y. (2021). A review of NMR analysis in polysaccharide structure and conformation: Progress, challenge and perspective. *Food Research International, 143*, Article 110290. https://doi.org/10.1016/j.foodres.2021.110290

Zeng, S., Long, J., Sun, J., Wang, G., & Zhou, L. (2022). A review on peach gum polysaccharide: Hydrolysis, structure, properties and applications. *Carbohydrate Polymers, 279*. https://doi.org/10.1016/j.carbpol.2021.119015

Zhang, H., Li, C., Ding, J., Lai, P. F. H., Xia, Y., & Ai, L. (2020). Structural features and emulsifying stability of a highly branched arabinogalactan from immature peach (*Prunus persica*) exudates. *Food Hydrocolloids, 104*, Article 105721. https://doi.org/10.1016/j.foodhyd.2020.105721

Zhang, T., Yang, Y., Liang, Y., Jiao, X., & Zhao, C. (2018). Beneficial effect of intestinal fermentation of natural polysaccharides. *Nutrients, 10*(8). https://doi.org/10.3390/nu10081055

Zhou, H., Wang, Z., Ma, H., Wang, S., Xie, W., Chen, Y., Xie, C., Guo, A., Wang, C., & Zheng, M. (2022). Characterisation and antioxidant activity of polysaccharide iron (III) complex in Qingzhuan Dark Tea. *Food Science and Technology, 42*, Article e119421. https://doi.org/10.1590/fst.119421